Arab J Sci Eng (2017) 42:3761–3777
DOI 10.1007/s13369-017-2461-y

RESEARCH ARTICLE - CIVIL ENGINEERING

An Analytical Research on Determination of Beam and Column Contribution to Plastic Energy Dissipation of RC Frames

Onur Merter[1] · **Taner Ucar**[2]

Received: 13 November 2015 / Accepted: 6 March 2017 / Published online: 17 March 2017

Abstract Determination of capacities of structural members, both in terms of strength and deformation, and estimation of seismic demand are essential issues in earthquake-resistant design. In energy-based design and evaluation, both the structural capacity and the demand imposed by earthquake are considered in terms of energy and accordingly energy dissipation capacity of the structure is associated with seismic energy demand. Plastic energy dissipation of structures under monotonic lateral loading may be obtained by using the resultant pushover curves of nonlinear static analyses. However, the time variation of individual contribution of structural members to the dissipated plastic energy cannot be determined. In this study, the contribution of beam and column deformations to the plastic energy dissipated in multistory reinforced concrete (RC) frames is determined by using nonlinear time history (NLTH) analysis. It is found that rotational deformations of beams are dominant in plastic energy dissipation. Accordingly, some linear relations considering the contribution of dissipated plastic energy in beam plastic hinges to the total plastic energy dissipation of RC frames are derived. Pushover analysis of frames in conducted and the area under the resultant pushover curve is determined to satisfy the mean value of the maximum plastic energy dissipated in frames during the selected earthquakes. The interstory drift ratios are calculated and compared with the interstory drift ratios directly obtained from NLTH analyses. The results are evaluated and presented by graphs and tables.

Keywords Plastic energy · Nonlinear time history analysis · Nonlinear static pushover analysis · Plastic hinges · Plastic energy contribution · Interstory drift ratio

1 Introduction

Structures are designed to withstand severe earthquakes which are expected to occur rarely during their economical lives. Although earthquake-resistant structures may experience moderate or heavy damages, the crucial aspect of seismic design is to prevent the total collapse of structures and unreasonable failure modes, such as soft-story or local failure mechanism. Strength, displacement and energy-based methods are currently used in earthquake-resistant design and evaluation of structures. Since structural damage is associated with irrecoverable hysteretic energy (i.e., plastic strain energy), a promising way for determination of structural damage in nonlinear behavior is the use of energy-based methods among these methods [1,2]. The use of energy concepts in earthquake-resistant structural design is first introduced by Housner, and the energy dissipated by linear elastic and nonlinear behavior of structural systems, the maximum energy of the structures and energy-based limit design issues are widely emphasized and demonstrated [3].

Earthquake effect is considered as energy input to the structure in energy-based design methods, and it is investigated whether the structural energy dissipation capacity is sufficient to meet earthquake energy demand or demand exceeds capacity. Since nonlinear properties of structural elements directly affect many characteristics of the whole structure such as ductility, displacement and energy demand,

✉ Onur Merter
onur.merter@deu.edu.tr

Taner Ucar
taner.ucar@deu.edu.tr

[1] Department of Civil Engineering, Dokuz Eylul University, Tinaztepe Campus, 35160 Izmir, Turkey

[2] Department of Architecture, Dokuz Eylul University, Tinaztepe Campus, 35160 Izmir, Turkey

plastic hinge mechanism and energy dissipation capacity, effective design of structural elements under earthquake impacts is a substantial matter. Cross-sectional dimensions and geometry, longitudinal and transverse reinforcement ratios and details, material strengths, plastic hinge length and external loads acting on members are the main parameters having an impact on nonlinear energy dissipation of structural members, and in this manner, characteristics of members have a great importance on determination of energy dissipation of structural systems in nonlinear behavior. Seismic energy demands on structures also depend on nonlinear properties of structural elements. The rotational hysteretic behavior of beam and column members and additional plastic axial deformations of columns under earthquake loading have a direct influence on seismic energy demand, as well as energy dissipation capacity of structures. The frequently used analysis method for the determination of earthquake input energy and energy demand is nonlinear time history (NLTH) analysis.

There are some important prior studies in the literature up till 2000s about the energy-based structural design and evaluation. They usually deal with determination of seismic energy dissipation in structural members and systems subjected to different types of loading and use of energy parameter as a structural design criterion [4–11]. Also, in the last decade the use of energy concept in earthquake and structural engineering had received wide press coverage through scientific researches. The major part of these researches constitutes of structural dynamic analyses, energy-based concepts and design and evaluation methods. Nonlinear dynamic analyses and hysteretic energy demands of RC frames are widely investigated in many studies [12–14]. Relevance of absolute and relative energy content in seismic evaluation of structures is discussed in detail by Kalkan and Kunnath [15]. The energy balance approach based on multimode pushover analysis to estimate seismic demands of buildings is researched by Jiang et al. [16]. Seismic input energy is expressed in Benavent-Climent by creating the design energy input spectra based on Colombian earthquakes [17]. Plastic design procedure is used in Terapathana's study considering the energy balance equality of frame structures [18]. The energy-based procedure is used to obtain target displacements of RC structures by Massumi and Monavari [19]. The energy-based design is dealt with in Habibi et al. [20] for seismic retrofitting. The new energy-based approach is used to predict the seismic demands of steel moment resisting frames subjected to near fault ground motions by Enderami et al. [21]. Energy dissipation of RC and steel members under different loadings is widely investigated in many different researches [22–26]. Some performance-based plastic design procedures are developed [27–31] in some studies. The seismic energy demand on structures is defined in the form of input and plastic energy demand spectra in Dindar et al. [32]. Input and hysteretic energy spectra for far-source ground motions, different hysteresis models and different ductility levels are investigated in Mezgebo and Lui [33]. An investigation is made by Hernandez-Montes et al. [34] considering energy components in nonlinear dynamic response of SDOF systems. Hysteretic energy, as the main seismic energy component, is analyzed and expressed by the spectrum in nonlinear systems as the ratio of hysteretic energy to input energy by Akbaş et al. [35].

Although there have been many studies in the literature about the determination of total plastic and hysteretic energy dissipations in structures due to earthquake excitations, there are not many researches which directly calculate the ratio of plastic energy dissipation in structural members such as beam and columns in a frame structure. Accordingly, in this study, plastic energy dissipation of five-story RC frames under the selected earthquakes is calculated by means of NLTH analysis. Plastic energy values corresponding to each time steps of ground motion are determined, and accordingly time variation of plastic energy is obtained graphically for the structures. Plastic energy contribution ratios of beams and columns are determined separately and presented in graphs where the contributions of rotational deformations of beams and columns and axial deformations of columns to dissipated plastic energy are also shown. It is found that the most contribution to the total dissipated plastic energy originates from rotational deformations of beam members. Accordingly, the correlation of the plastic energy dissipated in beam plastic hinges with the total plastic energy dissipation of frames yields some equations obtained from regression analysis. Finally, the mean values of the maximum plastic energies dissipated during the considered earthquakes are indicated as an area in pushover curves. Interstory drift ratios which correspond to mean of dissipated plastic energies are compared to the interstory drift values from NLTH analysis.

2 Idealization of Cyclic Behavior of Structural Members and Plastic Energy Definition

The plastic energy, which is defined as the energy dissipation during nonlinear behavior, may be thought as classical work–energy principle. Accordingly, for a bending member subjected to an earthquake excitation, the plastic energy is formulated as in Eq. (1):

$$E_{\mathrm{pi}} = \left| M_{\mathrm{i}} \cdot \theta_{\mathrm{pi}} \right| \tag{1}$$

where M_{i} corresponds to bending moment at any time instant of earthquake, and E_{pi} is the plastic energy of the member.

Equation (2) yields the plastic rotation of the plastic hinge formed in ith sequence (θ_{pi}), where θ_{i} is the total rotation at any time instant of earthquake and θ_{yi} is the yield rotation.

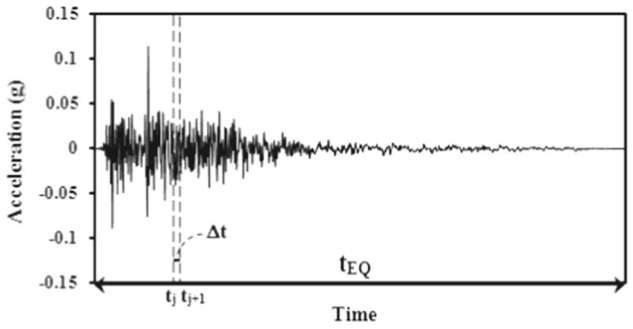

Fig. 1 Earthquake acceleration record sample

$$\theta_{\mathrm{pi}} = \theta_{\mathrm{i}} - \theta_{\mathrm{yi}} \tag{2}$$

Equation (1) may be rewritten as in Eq. (3) for a certain ground motion time "t".

$$E_{\text{pi-beam}}\,(M-\theta) = \left|M_{\mathrm{i}}\,(t)\cdot\theta_{\mathrm{pi}}\,(t)\right| \tag{3}$$

where $E_{\text{pi-beam}}(M-\theta)$ is the time-dependent plastic energy expression of a structural member, $M_{\mathrm{i}}(t)$ and $\theta_{\mathrm{pi}}(t)$ are the bending moment and plastic rotation at any time instant t, respectively.

While the number of total recorded strong ground motion is indicated by "m" and the time interval for subsequent acceleration records is shown by "Δt" ($t_{j+1}-t_j$), the duration of an earthquake ground motion (t_{EQ}) can be written as:

$$t_{\mathrm{EQ}} = \Delta t\cdot(m-1) \tag{4}$$

The above explained terms are shown on an earthquake acceleration record sample in Fig. 1.

The total plastic energy dissipated in plastic hinges in RC beam and column members of a frame structure under seismic effects may be expressed as:

$$\begin{aligned} &E_{\text{pi-beam}}\,(M-\theta) + E_{\text{pi-column}}\,(M-\theta)\\ &\quad=\sum_{i=1}^{i=n}\left(\sum_{t=0}^{t=\Delta t(m-1)}\left|M_{\mathrm{bi}}\,(t)\cdot\theta_{\mathrm{pbi}}\,(t)\right|\right)\\ &\qquad+\sum_{i=1}^{i=k}\left(\sum_{t=0}^{t=\Delta t(m-1)}\left|M_{\mathrm{ci}}\,(t)\cdot\theta_{\mathrm{pci}}\,(t)\right|\right) \end{aligned} \tag{5}$$

where $E_{\text{pi-beam}}(M-\theta)$ is the total plastic energy dissipated in beam plastic hinges subjected to pure bending, and $E_{\text{pi-column}}(M-\theta)$ is the total plastic energy dissipated in column plastic hinges under combined bending and axial load. In Eq. (5), the subscripts b and c stand for beam and column, respectively, n is the total number of plastic hinges in beams ($i=1$ to n) and k is the total number of plastic hinges in columns ($i=1$ to k). $t=\Delta t(m-1)$ corresponds to the duration of a ground motion. $M_{\mathrm{bi}}(t)$, $\theta_{\mathrm{pbi}}(t)$, $M_{\mathrm{ci}}(t)$ and $\theta_{\mathrm{pci}}(t)$ are the moment and plastic rotation values of beam and column plastic hinges, respectively, as functions of earthquake motion time (t).

Column plastic hinges may form for many different ($M_{\mathrm{ci}}-N_{\mathrm{ci}}$) couples on interaction diagrams, which define the capacity of column members. If axial deformations of columns are considered in plastic energy calculations, the total plastic energy may be written as follows:

$$\begin{aligned} \sum E_{\text{p,frame}}\,(t) &= \sum_{i=1}^{i=n}\left(\sum_{t=0}^{t=\Delta t(m-1)}\left|M_{\mathrm{bi}}\,(t)\cdot\theta_{\mathrm{pbi}}\,(t)\right|\right)\\ &\quad+\sum_{i=1}^{i=k}\left(\sum_{t=0}^{t=\Delta t(m-1)}\left|M_{\mathrm{ci}}\,(t)\cdot\theta_{\mathrm{pci}}\,(t)\right|\right)\\ &\quad+\sum_{i=1}^{i=k}\left(\sum_{t=0}^{t=\Delta t(m-1)}\left|N_{\mathrm{ci}}\,(t)\cdot\delta_{\mathrm{pci}}\,(t)\right|\right) \end{aligned} \tag{6}$$

In Eq. (6), $\theta_{\mathrm{pci}}(t)$ and $\delta_{\mathrm{pci}}(t)$ are the rotational and axial plastic deformation of column plastic hinges, respectively, $N_{\mathrm{ci}}(t)$ is the axial load corresponding to ($M_{\mathrm{ci}}-N_{\mathrm{ci}}$) couple which forms plastic hinge in the column, $\delta_{\mathrm{pci}}(t)$ is the axial plastic deformation of the column when the axial force is equal to $N_{\mathrm{ci}}(t)$ and $\sum E_{\text{p,frame}}\,(t)$ is the total plastic energy of RC frame structure. The dissipated plastic energy in the column [the last two terms of Eq. (6)] is the function of $M_{\mathrm{ci}}(t)$, $\theta_{\mathrm{pci}}(t)$, $N_{\mathrm{ci}}(t)$ and $\delta_{\mathrm{pci}}(t)$($E_{\text{pi-column}} = f[M_{\mathrm{ci}}(t),\ \theta_{\mathrm{pci}}(t),\ N_{ci}(t),\ \delta_{\mathrm{pci}}(t)]$). Different ($M_{\mathrm{ci}}-N_{\mathrm{ci}}$) couples, which cause to form a plastic hinge in columns, are shown in the interaction diagram in Fig. 2, where ε_{s} and $\varepsilon'_{\mathrm{s}}$ are the reinforcement strains in tension and compression, respectively, and $\varepsilon_{\mathrm{cu}}$ is the ultimate strain value of the exterior concrete fiber in compression.

Rewriting the plastic energy equality for RC frame in Eq. (6) in general form yields Eq. (7):

$$\begin{aligned} \sum E_{\text{p,frame}}\,(t) &= E_{\text{pi-beam}}\,(M-\theta)\\ &\quad+E_{\text{pi-column}}\,(M-\theta)\\ &\quad+\sum\left|N_c\cdot\delta_{\mathrm{pc}}\right| \end{aligned} \tag{7}$$

where $\sum\left|N_{\mathrm{c}}\cdot\delta_{\mathrm{pc}}\right|$ corresponds to the general term of $\sum_{i=1}^{i=k}\left(\sum_{t=0}^{t=\Delta t(m-1)}\left|N_{\mathrm{ci}}\,(t)\cdot\delta_{\mathrm{pci}}\,(t)\right|\right)$ in Eq. (6). The total plastic energy dissipation of a frame ($\sum E_{\text{p,frame}}\,(t)$) may be separated to two parts; $E_{\text{pi-beam}}\,(M-\theta)$ indicates the contribution of beam members to the total plastic energy dissipation of a frame, and $E_{\text{pi-column}}\,(M-\theta)+\sum\left|N_{\mathrm{c}}\cdot\delta_{\mathrm{pc}}\right|$ corresponds to the contribution of column members to the

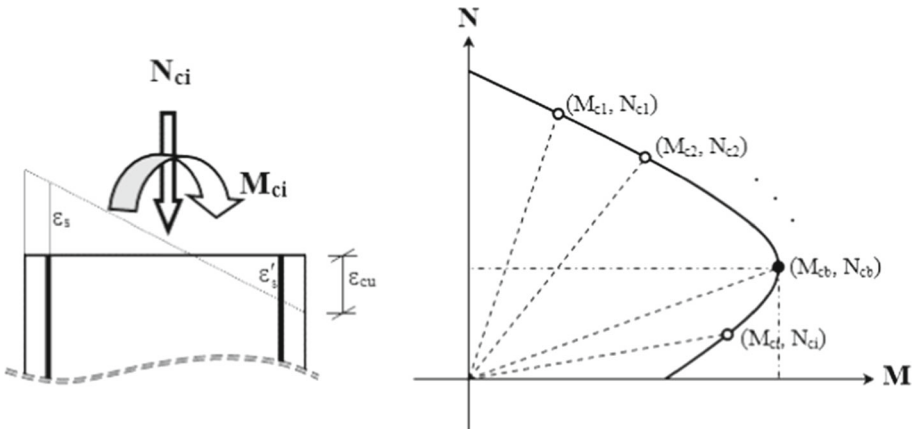

Fig. 2 Cross section of RC column, strain and interaction diagrams

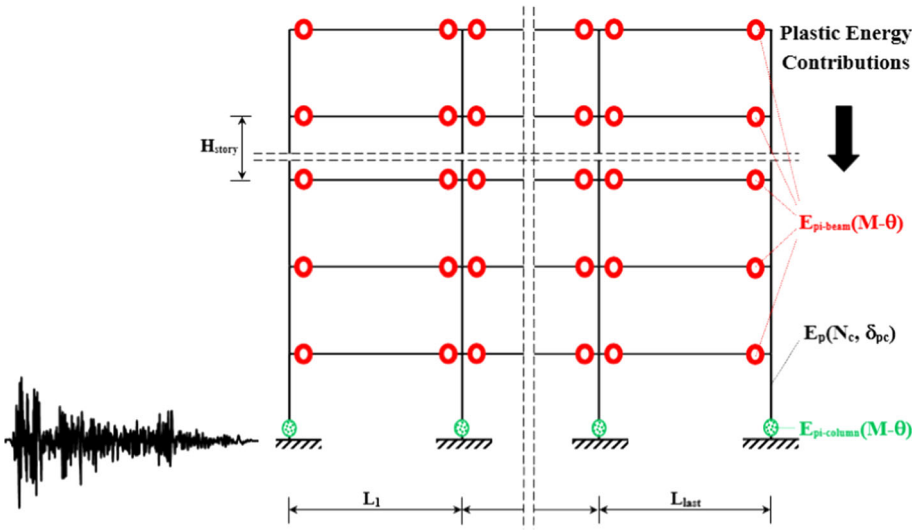

Fig. 3 Sample plastic hinge mechanism and plastic energy dissipation

total plastic energy dissipation in a frame due to nonlinear behavior.

A sample plastic hinge mechanism of RC multistory frame structure which is affected by a strong ground motion and plastic energy distribution is shown in Fig. 3, where L_1 is the first span, L_{last} is the last span and H_{story} is the story height. Beam plastic hinges are expressed by red circles, whereas column plastic hinges are expressed by green circles in the figure. The sum of plastic energy dissipated in beam and column plastic hinges in Fig. 3 gives the plastic energy dissipation of the whole frame ($\sum E_{\text{p,frame}}(t)$) which is indicated by Eq. (7).

3 Determination of Plastic Energy and Contribution of Structural Members

Estimation of the earthquake plastic energy dissipation of structures having certain plastic energy capacity is a substantial issue in energy-based structural design and evaluation. The total plastic energy dissipation of the frame structure in nonlinear behavior, which is expressed by Eq. (7), is determined graphically within the study. The plastic energy–time ($E_p - t$) graphs of frames are obtained from NLTH analysis. The maximum plastic energy dissipated during an earthquake ($E_{\text{p,max}}$) may be determined by using these graphs expressing time-dependent variation of plastic energy dissipation. A representative plastic energy–time ($E_p - t$) graph of a multistory frame structure is shown in Fig. 4.

The maximum plastic energy dissipated during an earthquake ($E_{\text{p,max}}$) determined from NLTH analysis may be associated with pushover curves of the structures obtained from monotonic nonlinear static analyses. Plastic energy dissipation in multistory structures during an earthquake is converted to monotonic-type (plastic) energy taking only positive values. The definition of maximum plastic energy ($E_{\text{p,max}}$) as an area in pushover curve is shown in Fig. 5, where the displacement δ corresponds to the maximum plastic energy in the pushover curve.

In the study, all of the plastic energy is assumed to be dissipated only in the plastic hinges. The dissipation of plastic energy can be achieved through rotational deformations of beam plastic hinges, whereas both rotational and axial deformations of column plastic hinges may contribute to

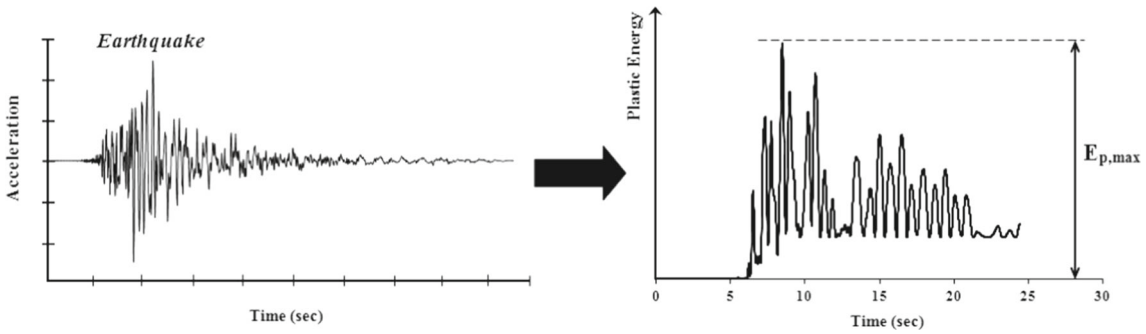

Fig. 4 Earthquake record and representative plastic energy demand graph

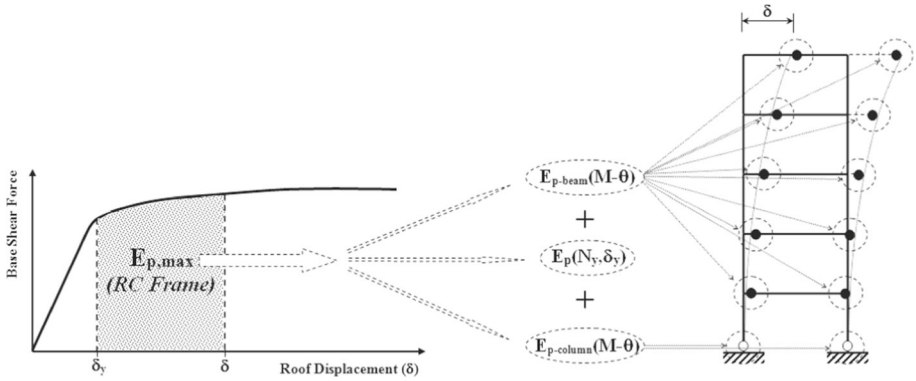

Fig. 5 Schematical expression of plastic energy in pushover curve and energy dissipation

plastic energy dissipation. Accordingly, the contribution of beam and column members to the plastic energy dissipation in frame structures is also investigated. Plastic energy dissipated by rotational deformations of beam and column plastic hinges and the contribution of axial plastic deformations to plastic energy dissipated in column plastic hinges are determined separately by means of NLTH analyses. The calculated energy contribution values of RC structural members are shown in plastic energy–time ($E_p - t$) graphs, and plastic energy dissipated in beam and column plastic hinges is practically obtained by using these graphs (Fig. 6). The contribution of rotational deformations of beam and column plastic hinges and the contribution of axial deformations of column plastic hinges to the total plastic energy dissipation are also shown on the same graph.

A proportional distribution (almost a linear relationship) between the dissipated plastic energy in frame and the plastic energy dissipated in beam plastic hinges is observed from Fig. 6. This observation leads to investigate a relation which can be suited for practical use in estimation of the plastic energy dissipated in a frame structure considering the plastic energy dissipated by rotational deformations of beam plastic hinges. Accordingly, the relationship between the dissipated plastic energy in frame ($\sum E_{p,frame}$) and the plastic energy dissipated only in beam plastic hinges ($\sum E_{p,beam}$) is assumed to be almost linear (Fig. 7). This assumption may vary due to characteristics of frame and its structural members and the sequence of plastic hinge formation. In

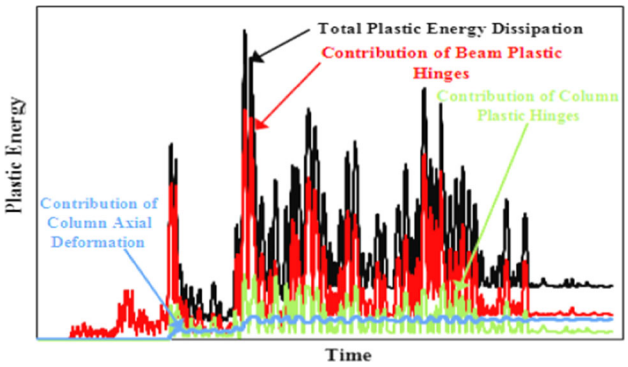

Fig. 6 Plastic energy contribution graph

code-designed RC frame structures having regular distributions in their mass and stiffness, where plastic hinges concentrate first at beam ends and then at the bottom end of ground columns, the significant contribution to the total plastic energy dissipated in the frame comes from beam plastic hinges. Equation (9) is used in order to introduce the linearity between the total plastic energy dissipated in frame and the plastic energy dissipated only in beam plastic hinges.

$$\sum E_{p,frame} \cong m \sum E_{p,beam} \left(\sum E_{p,frame} \alpha \sum E_{p,beam} \right)$$
$$\text{or} \sum E_{p,frame} \cong m \sum E_{p,beam} + n \qquad (8)$$

Equation (9) gives the slope of the line which represents the linear relationship between the dissipated plastic energy

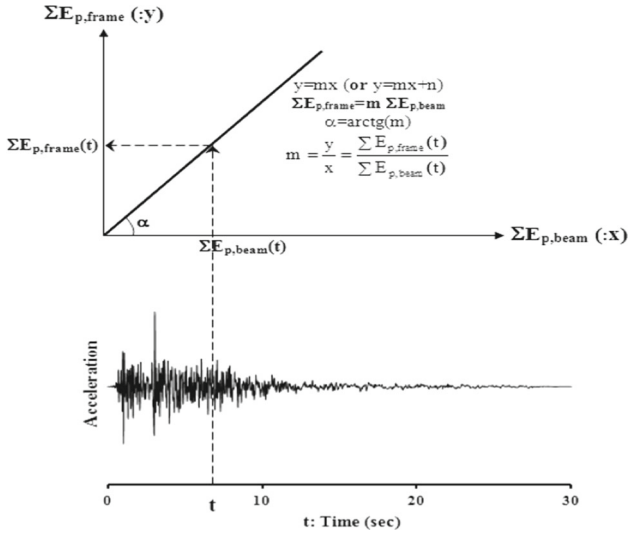

Fig. 7 Relationship of plastic energy dissipated by beams and frame

in frame and the plastic energy dissipated in beam plastic hinges.

$$m \cong \frac{\sum E_{\text{p,frame}}(t)}{\sum E_{\text{p,beam}}(t)} \tag{9}$$

4 Case Study

In the presented work, the amount of plastic energy dissipated in 5-story one-, three- and five-bay regular RC frame structures are determined as a result of performed NLTH analysis. The selected frames are abbreviated considering the number of stories and bays. The abbreviations of 5-story one-, three- and five-bay RC frames are as RCF5-1, RCF5-3 and RCF5-5, respectively.

4.1 Reinforced Concrete Design of Frames

Material properties are assumed to be 25 MPa for the concrete compressive strength and 420 MPa for the yield strength of both longitudinal and transverse reinforcements. There exist uniformly distributed dead (G) and live (Q) loads in all spans and concentrated dead (P_G) and live (P_Q) loads in columns. Uniformly distributed dead and live loads are assumed to be 34.50 and 14.00 kN/m, respectively. Concentrated dead and live load of the corner columns of frames is 135 kN and is 35 kN, respectively. Concentrated dead and live load of the interior columns of RCF5-3 and RCF5-5 is 170 kN and is 70 kN, respectively. All frames are assumed to be on the Seismic Zone 1, and the Local Site Class is taken as Z3 according to TSDC [36]. According to the average of shear wave velocity in the first 30 m of the soil (V_{S30} values), soil profile type definitions of Z3 may be considered as the counterparts of soil profile types S_D in UBC-97 [37] and C in Eurocode 8 [38].

Live load participation factor (n) is taken as 0.30, and floor weights and related masses, which are considered in seismic calculations, are determined as the combination of dead loads and 30% of live loads. Seismic masses are assumed to be lumped at the center of mass of each story.

The selected RC frame structures are designed and detailed to satisfy the requirements of Turkish Standards-TS500 [39] and TSDC considering both gravity and seismic loads. RC design of frames is performed using the structural analysis program SAP 2000 [40]. Geometrical properties of the frames and dimensions of beams and columns in cm are given in Fig. 8.

Dimensions and longitudinal reinforcement configurations of beam and column members of RCF5-1, RCF5-3 and RCF5-5 are shown in Figs. 9 and 10, respectively. Transverse reinforcements are chosen as closed stirrups with diameters

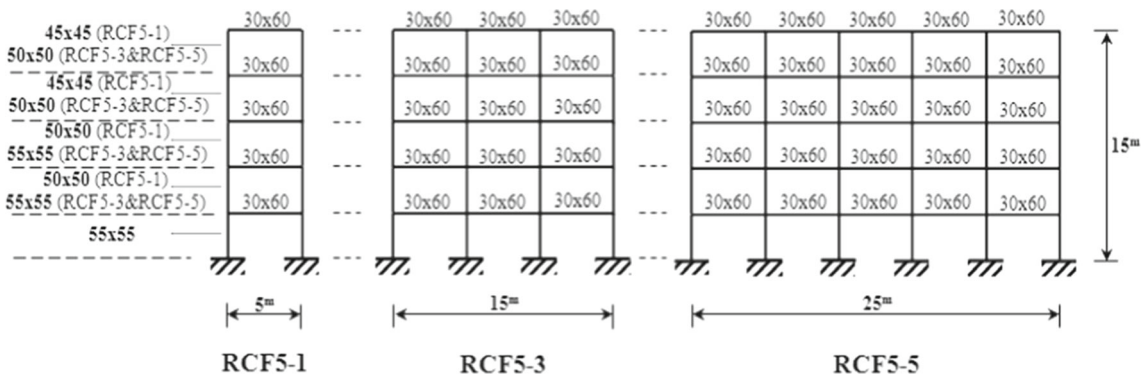

Fig. 8 5-Story RC moment resisting frames

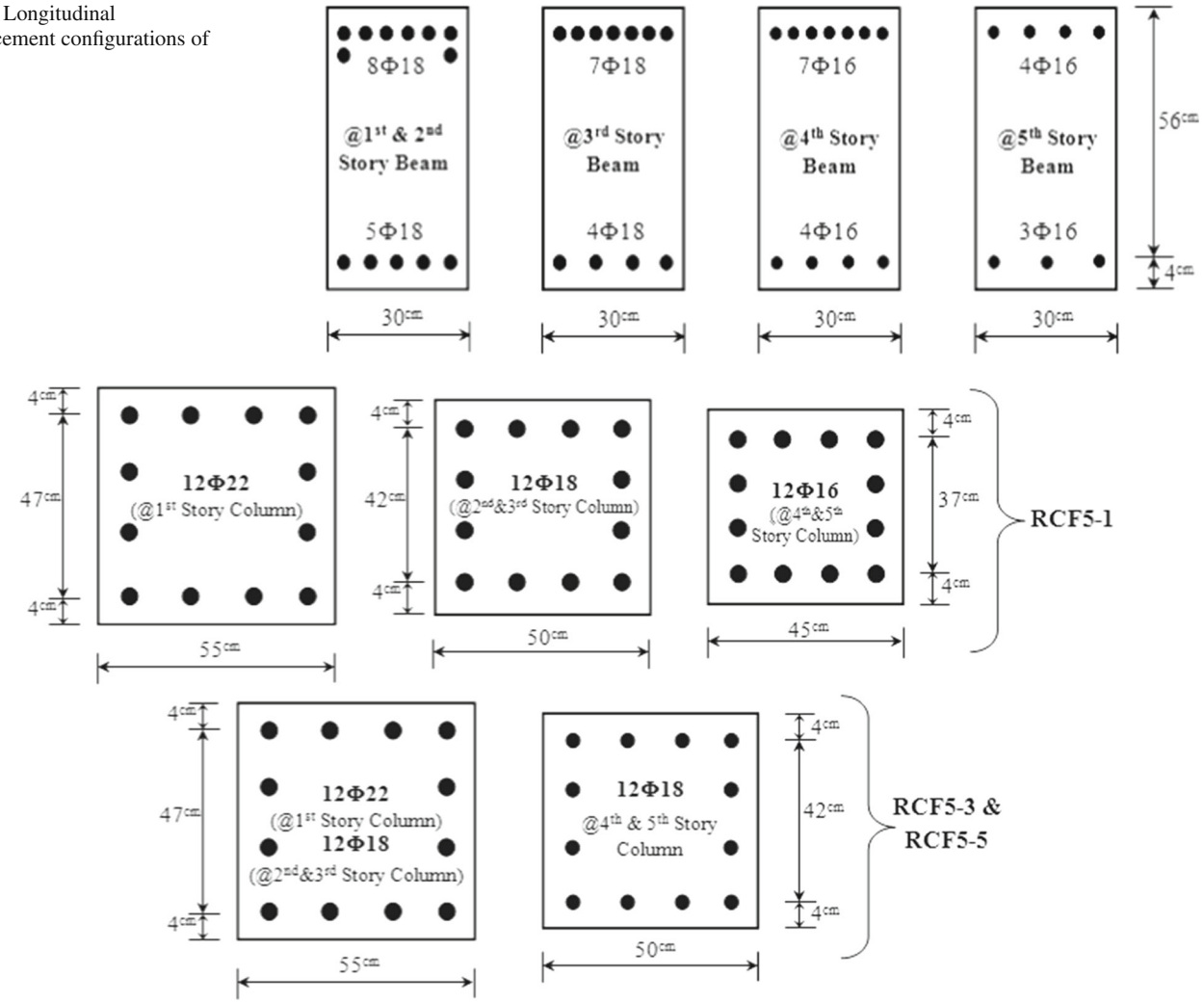

Fig. 9 Longitudinal reinforcement configurations of beams

Fig. 10 Longitudinal reinforcement configurations of columns

of 10 mm. The spacing of beam stirrups is 10 cm in confinement zones, which are designed with a length of twice the beam depth at both ends of beam according to TSDC and 15 cm in midspans. The spacing of column stirrups is 8 cm in confinement zones assuming at least 50 cm at both ends of the columns according to TSDC and 10 cm in midspans.

4.2 Nonlinear Modeling Aspects and Dynamic Analyses

Nonlinear dynamic analyses of the study are performed by using PERFORM 3D [41]. The structural models have already been created in SAP2000 environment, and elastic properties of structural members are imported directly from SAP2000 to PERFORM 3D. Each frame element is a line element with a linear elastic middle portion bounded by rigid hinges at member ends where inelastic properties are assigned.

Plastic hinge hypothesis (lumped plasticity model) is used to define inelastic behavior of the material. Stress–strain relations of TSDC are used for nonlinear modeling of concrete and steel reinforcement materials. Accordingly, the stress–strain relationships proposed by Mander et al. [42] are implemented for unconfined and confined concrete. Reinforcement steel is modeled by parabolic strain hardening steel model. Plastic hinges are accepted to form at both ends of the beam and column members. Moment versus plastic rotation ($M - \theta_p$) relations of structural members are obtained by using the program developed by the authors in Excel software. Plastic hinges are rigid-plastic. Plastic hinge length (L_p) is assumed to be the half of the cross-sectional depth due to its simplicity. The initial effective stiffness values of structural elements are reduced according to the TSDC in order to account for cracking in sections during the inelastic response of frames. Accordingly, the effective flexural stiffness of beams is taken as 40% of

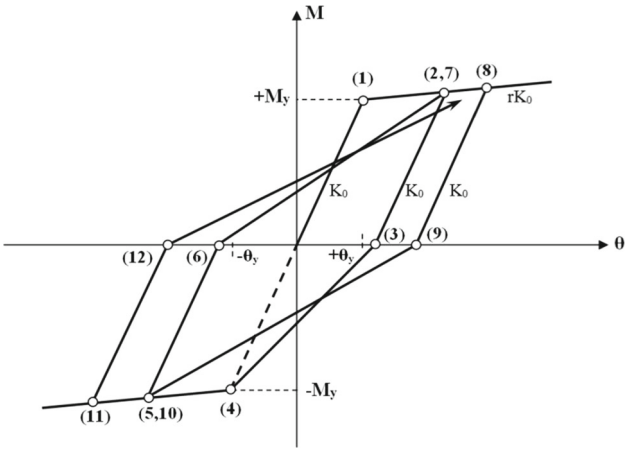

Fig. 11 Moment–rotation ($M-\theta$) relationship of the hysteretic model

the uncracked stiffness of the section. The effective flexural stiffness of columns ((EI)e) is taken to be between 40 and 80% of the uncracked stiffness ((EI)o) according to the level of axial load (i.e., if $N_D/(A_c f_c) \leq 0.10$ then (EI)e = 0.40(EI)o and if $N_D/(A_c f_c) \geq 0.40$ then (EI)e = 0.80(EI)o). For $N_D/(A_c f_c)$ between 0.10 and 0.40, a linear interpolation is performed. In these relations, N_D is axial load, A_c is cross-sectional area of the column and f_c is concrete compressive strength. Geometrical variations (i.e., the second-order effects) are taken into account. The shear capacity of each of beam and column members is calculated according to TS500 and is compared with those shear force values obtained from analyses. Since shear capacity of structural members is not exceeded, shear failure is not observed.

The modeling of cyclic behavior of structural members under seismic effects is a very important subject in earthquake engineering. Accordingly, the idealization of cyclic moment–rotation ($M-\theta$) relations of bending members is a critical issue in nonlinear analysis of RC structures. Many experimental researches to model the inelastic response of RC structural elements subjected to cyclic deformation reversals have been devoted. As a result of these studies, different idealized numerous moment–rotation relationships incorporating information from experimental investigations of the hysteretic behavior of RC structural elements have been proposed. Some of those theoretically and experimentally validated hysteretic models are Takeda model, the modified Clough model, Flag-Shaped model, bilinear models, etc., [43–48].

Since it affects the seismic behavior of a structure, the selection of a proper model to characterize the hysteretic behavior is important. Hysteretic models considering degradation of stiffness due to increasing damage are convenient for RC members. Moment–rotation relationships of the hysteretic model used in this study are shown in Fig. 11, where K_0 is initial stiffness, rK_0 is post-yield stiffness, and $\pm M_y$ and $\pm\theta_y$ are positive and negative yield moment and yield rotation, respectively. The post-yield stiffness is assumed to be 3% of the initial stiffness. The degradation in unloading stiffness is not considered, and accordingly the unloading stiffness is always equal to the initial elastic stiffness.

Nonlinear dynamic analyses of frames are performed by using the time histories of ten recorded earthquakes. The accelerograms for the earthquakes are constructed by using the data provided from the official Web site of the Pacific Earthquake Engineering Research Center [49]. Details of the ground motion records are given in Table 1, where M_w is the moment magnitude of earthquake, R_{JB} is the Joyner–Boore distance, V_{S30} is the average of shear wave velocity in the first 30 m of the soil, *PGA* is the peak ground acceleration, *PGV* is the peak ground velocity, and *PGD* is the peak ground displacement. Acceleration time histories of the selected earthquakes are shown in Fig. 12. The selected filtered ground motions have strike-slip fault mechanism, do not involve near fault effects and satisfy all the conditions given in TSDC.

Table 1 Details of ground motion records

EQ. no.	Earthquake and date	M_w	R_{JB} (km)	V_{S30} (m/s)	PGA (g)	PGV (cm/s)	PGD (cm)
1	Imperial Valley—15.10.1979	6.53	15.19	659.6	0.176	14.04	5.84
2	Kobe—16.01.1995	6.9	7.1	609	0.509	37.3	9.52
3	Parkfield—28.06.1966	6.19	17.64	408.9	0.063	6.8	3.55
4	Hector Mine—16.10.1999	7.13	10.35	684.9	0.306	34.21	17.71
5	Chi Chi (Taiwan)—20.09.1999	6.2	12.4	680	0.123	15.86	5.64
6	Duzce (Sakarya St.)—12.11.1999	7.14	45.2	471	0.023	5.5	7.34
7	Duzce (Mudurnu St.)—12.11.1999	7.14	34.3	659.6	0.12	9.3	7.63
8	Duzce (Lamont St.)—12.11.1999	7.14	23.4	517	0.042	9.2	8.07
9	Victoria (Mexico)—06.09.1980	6.33	13.8	659.6	0.621	31.6	13.2
10	Chalfant Valley—21.07.1986	6.19	29.4	338.5	0.064	3.79	1.26

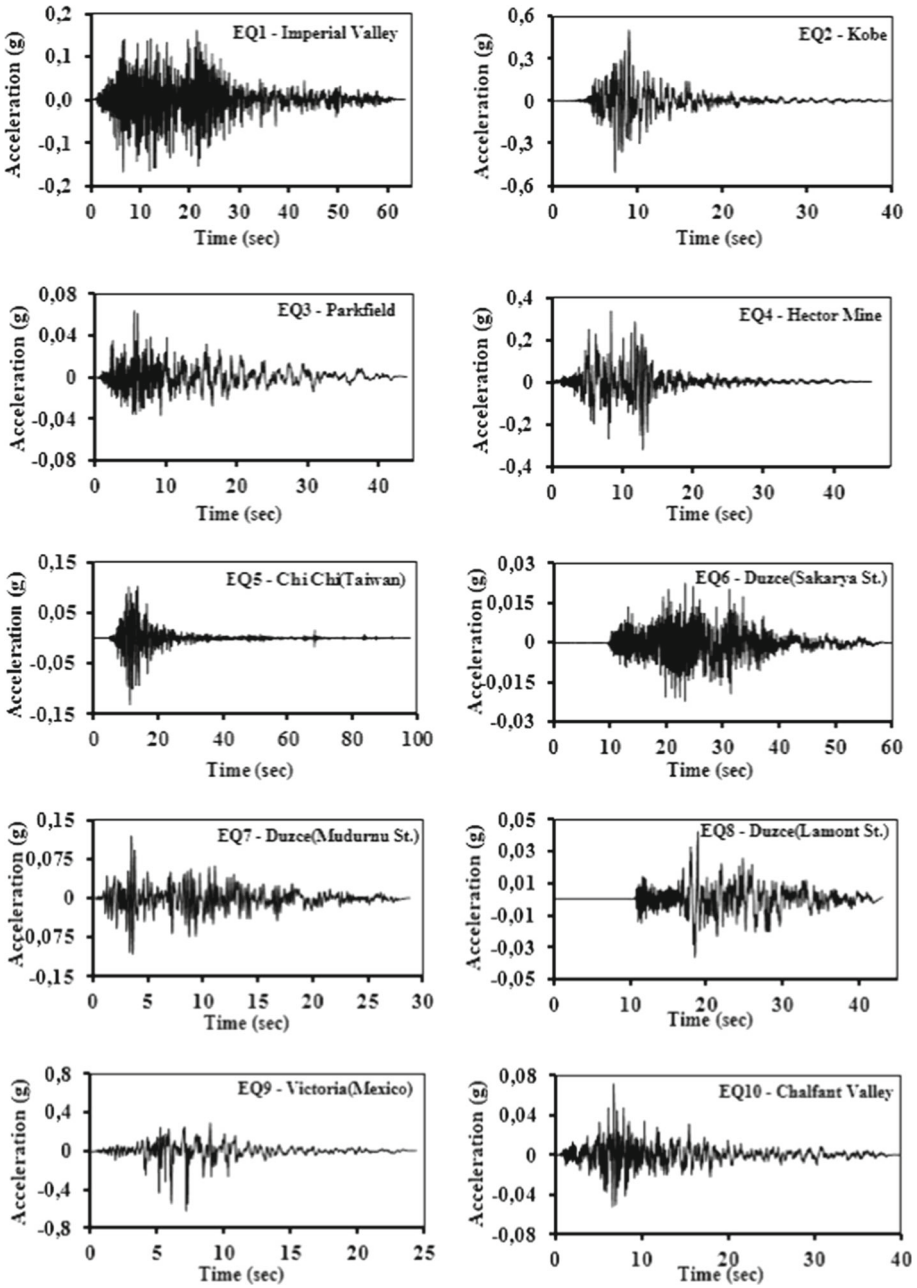

Fig. 12 Acceleration time histories of earthquakes

Records are scaled in time-domain considering Z3 acceleration spectrum of TSDC. The time-domain scaled and design spectrum compatible acceleration spectra of the selected ten ground motions are shown together with the design spectrum of TSDC for local site class Z3 in Fig. 13.

Nonlinear time history analyses are performed using the structural analysis program PERFORM 3D. Modal damping ratio is taken as 5% and Rayleigh damping model, which assumes that the damping is proportional to a linear combination of the stiffness and mass [50], and is used in dynamic analyses.

4.3 Contribution of Beam and Column Deformations to Plastic Energy Dissipated in RC Frames

The plastic energy dissipated in the selected 5-story RC frame structures subjected to different earthquakes is determined, and the results are presented graphically. In these graphical representations, the contribution of beam and column deformations to the total plastic energy dissipated in the RC frame structure for each time instant of the selected earthquakes is shown (Figs. 14, 15, 16). Plastic energy dissipation versus time graphs of RCF5-1 during earthquakes EQ3, EQ8 and EQ9 are shown in Fig. 14, while same graphs of RCF5-3

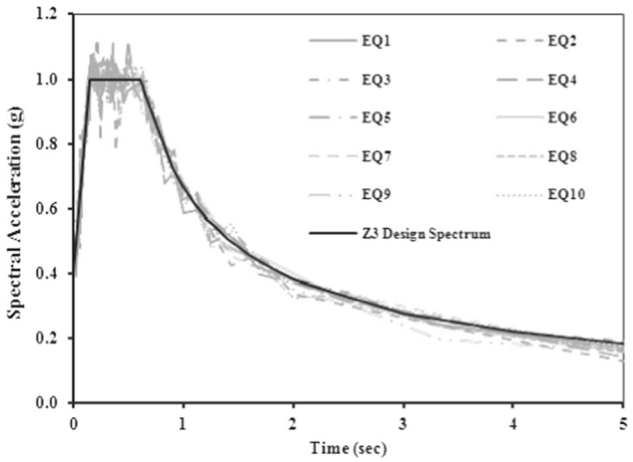

Fig. 13 Scaled acceleration spectra of earthquakes and elastic design spectrum of Z3

during earthquakes EQ2, EQ5, EQ6 and EQ9 are given in Fig. 15. Shown in Fig. 16 is plastic energy dissipation versus time graphs of RCF5-5 during earthquakes EQ1, EQ4, EQ7 and EQ10. Additionally, the contribution of rotational deformations of beam and column plastic hinges and the contribution of axial deformations of column plastic hinges to the total plastic energy are shown in Figs. 14, 15 and 16.

The maximum values of plastic energy dissipated in RC frame structures during the selected earthquakes are given in Table 2. The mean values of plastic energy obtained from NLTH analyses of the frames are 23.49, 44.72 and 81.45 kNm for RCF5-1, RCF5-3 and RCF5-5, respectively.

In Figs. 17, 18 and 19, the contribution ratios of rotational deformations of beam and column plastic hinges and the contribution of axial deformations of column plastic hinges to the total plastic energy dissipated in frames RCF5-1, RCF5-3 and RCF5-5 are shown. The contributions of rotational deformations of beam and column plastic hinges are represented by red and green straight lines, respectively, where the contribution of axial deformations of column plastic hinges is represented by a blue straight line. The plastic energy graphs may vary with characteristics of frames and earthquakes. The formation of plastic hinge mechanism directly influences the plastic energy dissipation. The contribution of beam hinges to the total dissipated plastic energy is generally high for the initial times of the earthquake, while it decreases later. When plastic hinges form in columns, in addition to rotational deformations axial deformations of column plastic hinges contribute to the total plastic energy. The contribution of both rotational and axial deformations of column plastic hinges to the total plastic energy dissipated in frames is considerably low at initial times of the earthquake, and then, it increases due to formation of plastic hinges in columns.

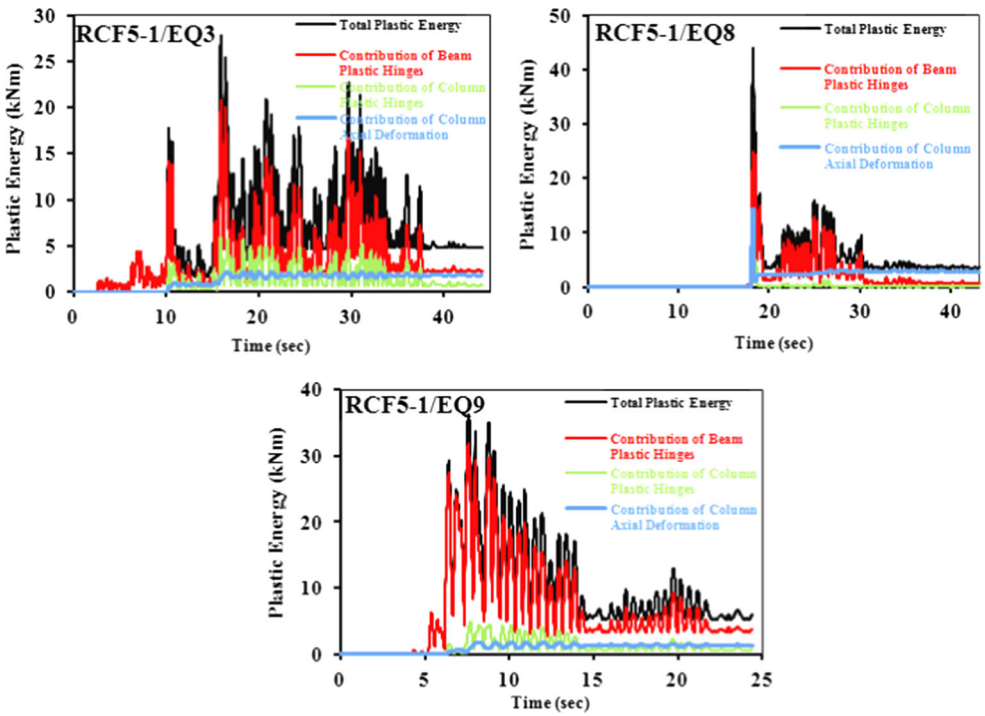

Fig. 14 Plastic energy dissipation versus time graphs of RCF5-1

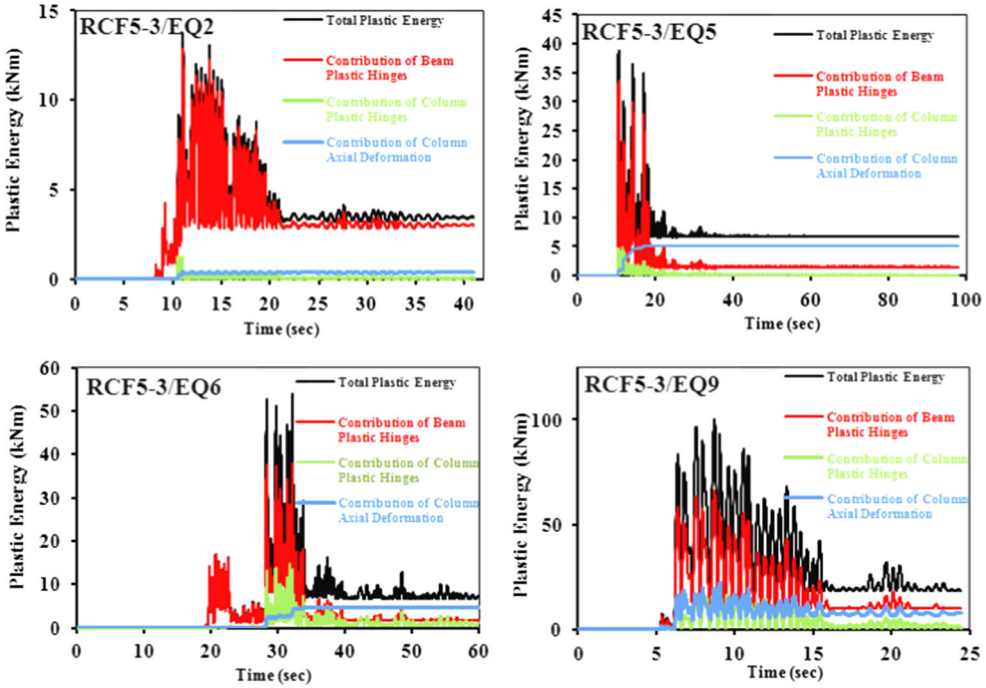

Fig. 15 Plastic energy dissipation versus time graphs of RCF5-3

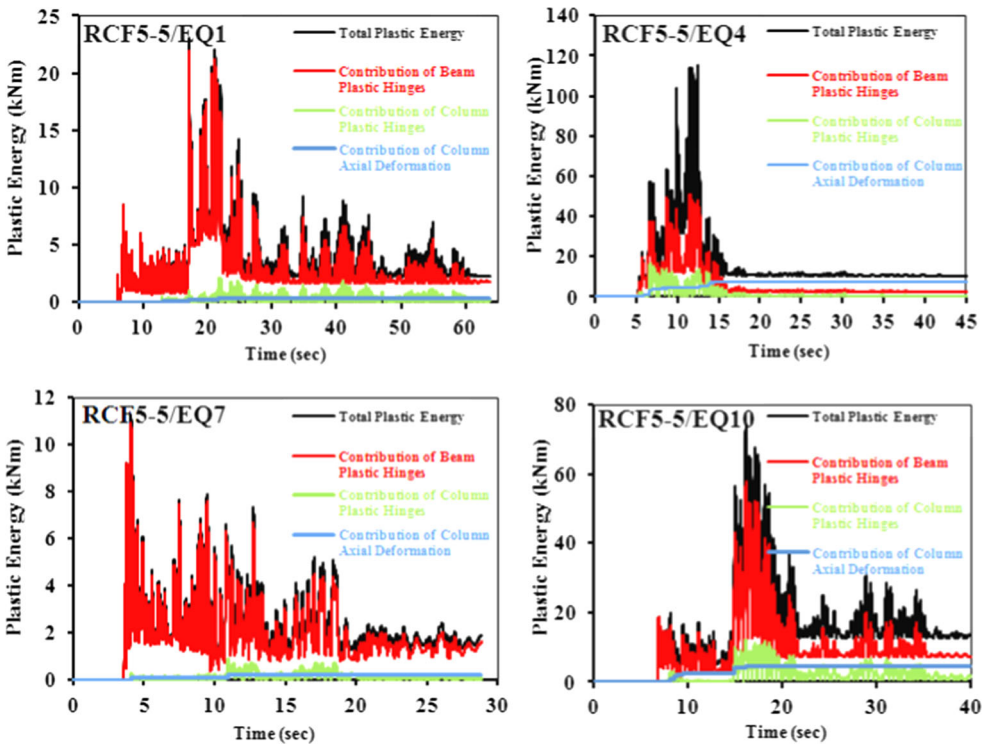

Fig. 16 Plastic energy dissipation versus time graphs of RCF5-5

Table 2 Maximum values of plastic energy dissipated in frames

Maximum plastic energy ($E_{p,max}$—kNm)			
Earthquakes	RCF5-1	RCF5-3	RCF5-5
EQ1	5.32	13.41	23.03
EQ2	3.00	11.03	73.89
EQ3	27.87	53.91	85.48
EQ4	48.02	71.21	115.27
EQ5	34.01	38.82	84.27
EQ6	10.50	54.09	100.88
EQ7	2.04	6.68	11.29
EQ8	43.98	57.42	89.92
EQ9	37.22	100.28	156.18
EQ10	22.89	40.36	74.33
Mean	23.49	44.72	81.45

4.4 Correlation of Plastic Energy Dissipated in Beam Hinges with Total Dissipated Plastic Energy

In the presented paper, which deals with the determination of the plastic energy dissipated in RC frames from NLTH analysis, the correlation of the plastic energy dissipated in beam plastic hinges with the total plastic energy dissipated in 5-story frame structures is also investigated. A linear model is fitted using regression analysis, and it is determined how well this linear model fits the data. The regression line does not miss any of the points by very much, so the R-squared (R^2) of the regression is relatively high which indicates how well data fit a statistical model. The coefficient of determination (R^2) and linear regression equations are shown in Fig. 20 for some of the selected ground motion records. In the linear regression equations, the variable y stands for the total plastic energy dissipated in the frame structure and the variable x stands for the contribution of beam plastic hinges.

The linear relation between the plastic energy dissipated in frame ($\sum E_{p,frame}$) and the contribution of beam plastic hinges ($\sum E_{p,beam}$) under the selected earthquakes is given by Eqs. (10–12) for RCF5-1, RCF5-3 and RCF5-5, respectively. The coefficients of linear Eqs. (10–12) are obtained as a result of the mean values of all earthquakes by using linear regression analyses.

$$\sum E_{p,frame} \cong 1.20\left(\sum E_{p,beam}\right) + 1.12 \tag{10}$$

$$\sum E_{p,frame} \cong 1.26\left(\sum E_{p,beam}\right) + 2.05 \tag{11}$$

$$\sum E_{p,frame} \cong 1.45\left(\sum E_{p,beam}\right) + 1.85 \tag{12}$$

It can be concluded that the linear regression equations of this study are valid only for the selected RC frame struc-

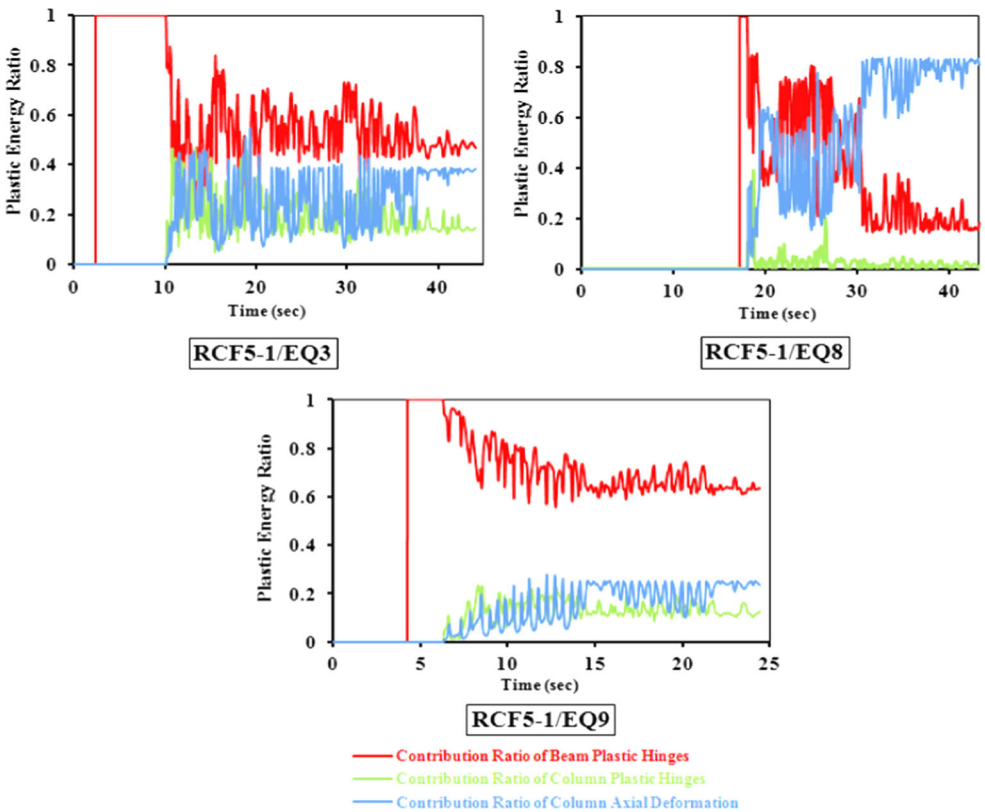

Fig. 17 Plastic energy dissipation ratio diagram of RCF5-1

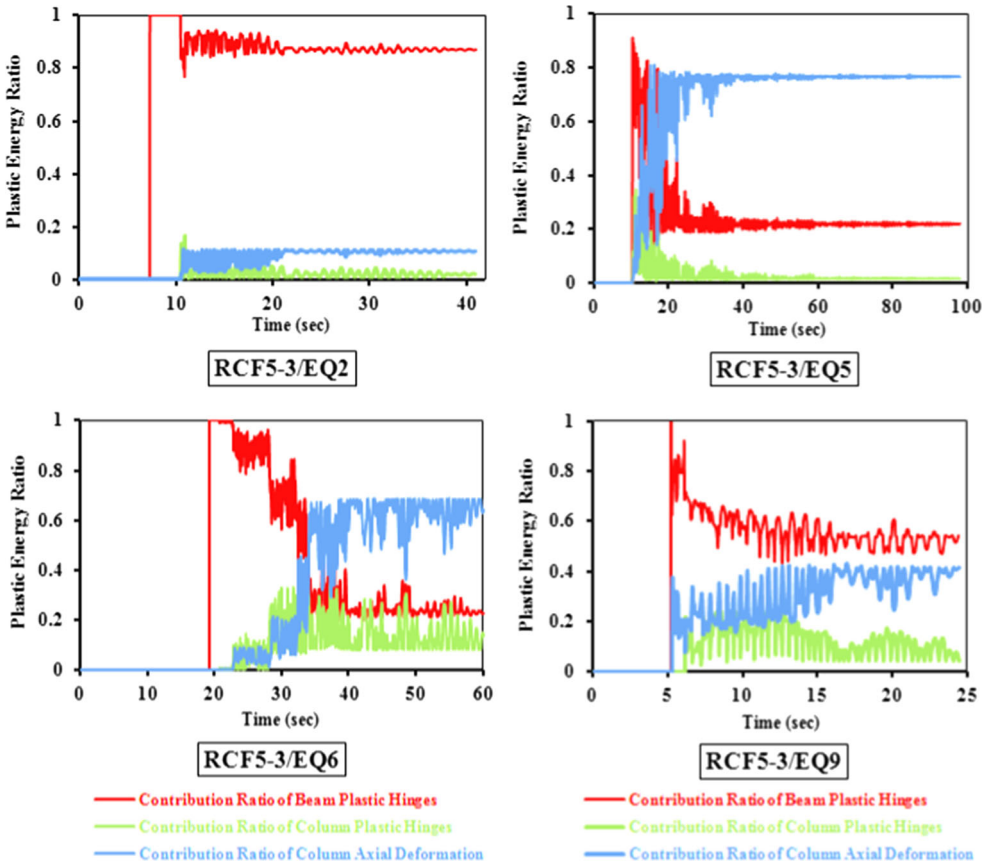

Fig. 18 Plastic energy dissipation ratio diagram of RCF5-3

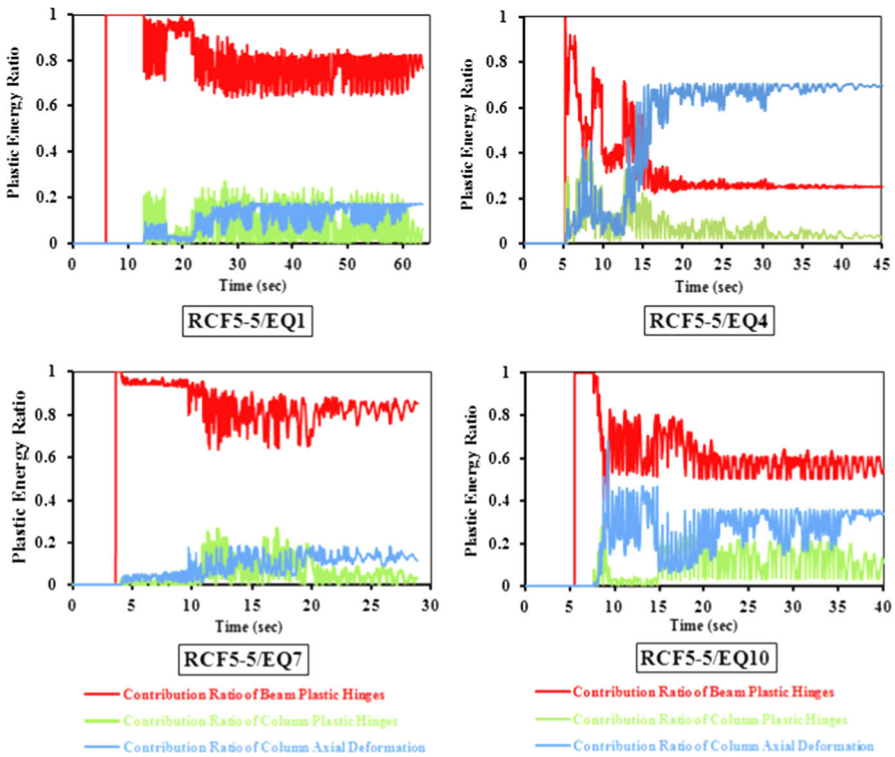

Fig. 19 Plastic energy dissipation ratio diagram of RCF5-5

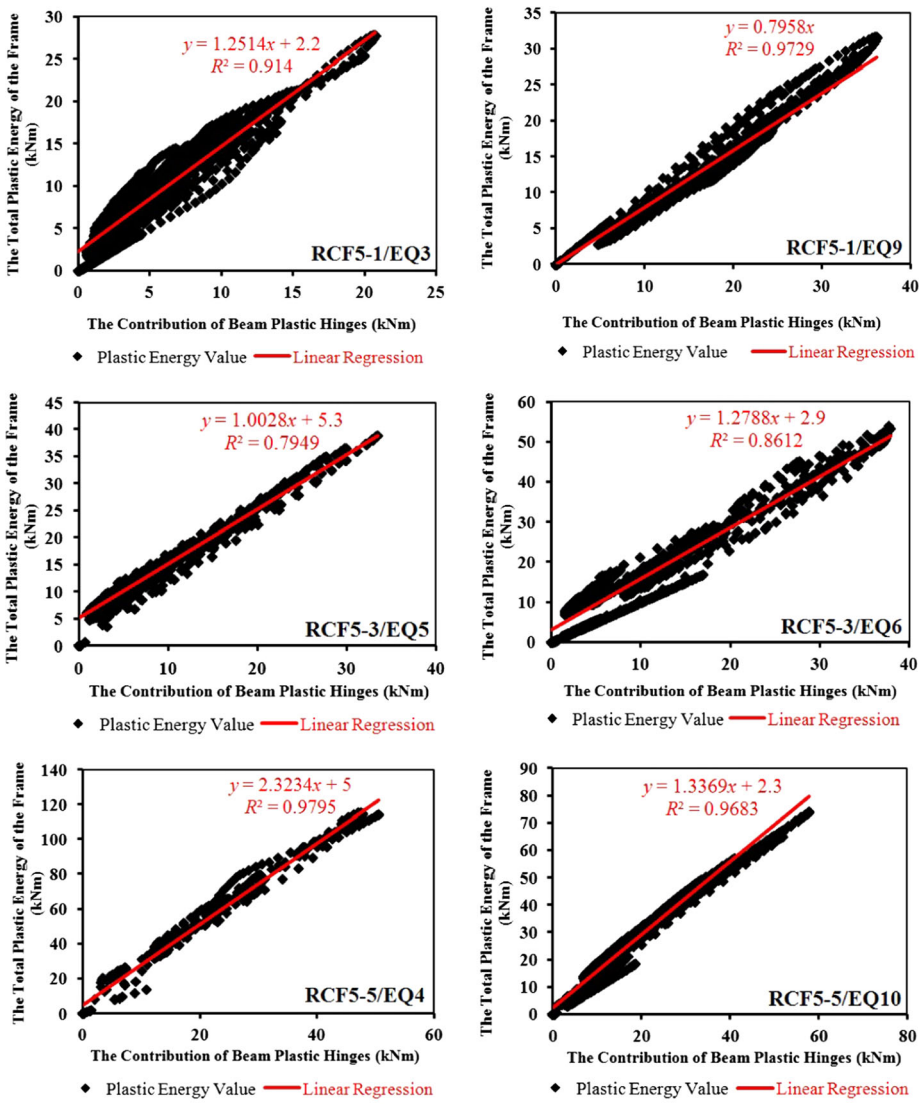

Fig. 20 Relation between plastic energy of frames and contribution of beam plastic hinges

tures and the used acceleration time histories. However, these equations may be used as simple formulas to determine the total plastic energy dissipated in regular RC frame structures which have similar sequence of hinge formation (i.e., global failure mechanism). For frames having different plastic hinge mechanism, the same linear relations may not be obtained.

4.5 Interstory Drift Ratios of the Frames

The rotation of the frame from the base (θ) corresponding to its maximum plastic energy can be approximated as follows:

$$\theta \cong \frac{\delta}{\sum H} \tag{13}$$

where δ is the lateral displacement of the top point of the frame which is assumed to be pushed statically up to satisfy the maximum plastic energy dissipation obtained from NLTH analysis ($E_{p,max}$). The parameters of Eq. (13) are shown in Fig. 21.

The shaded areas under the pushover curves in Fig. 22 are conveniently determined to give the mean values of the maximum plastic energy dissipated in frames during the selected

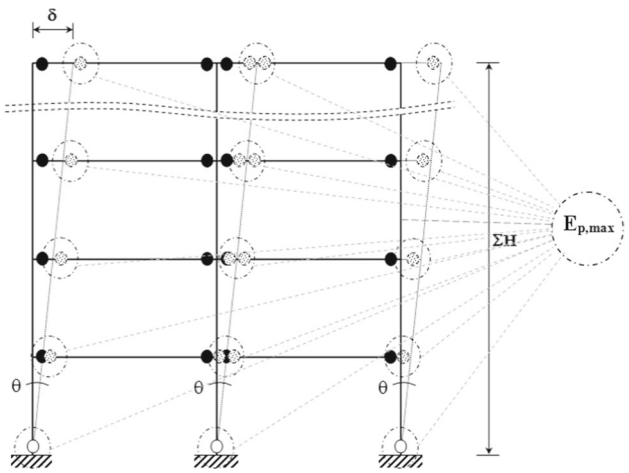

Fig. 21 A sample RC frame with plastic hinge mechanism

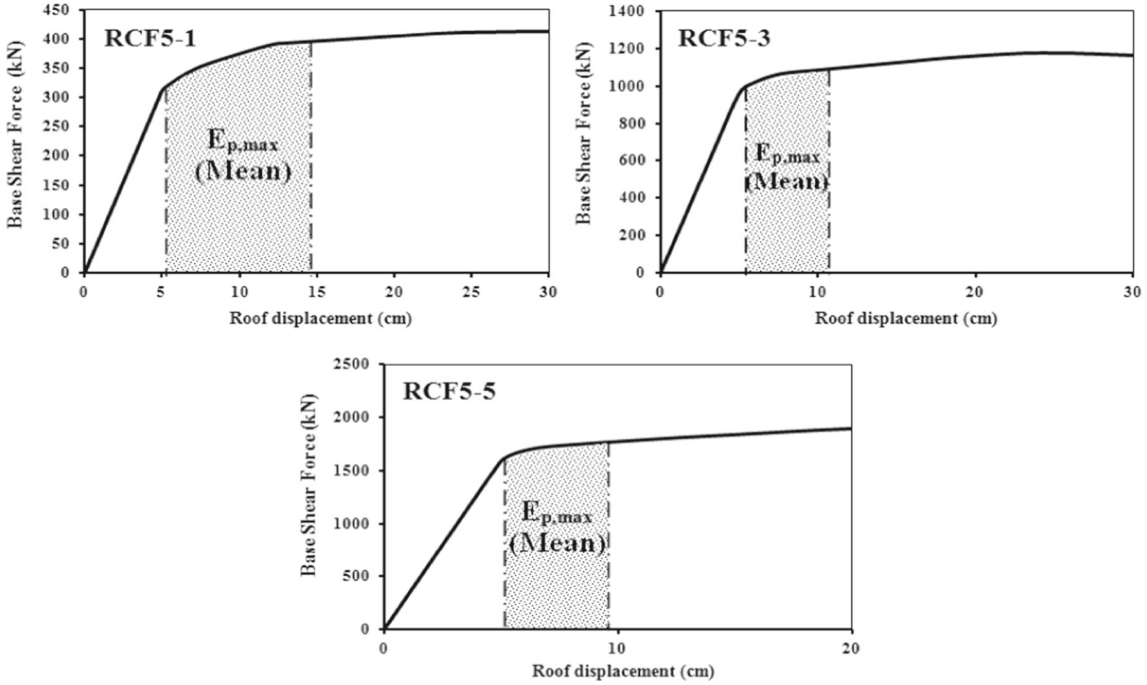

Fig. 22 Pushover curves of frames with $E_{p,max}$

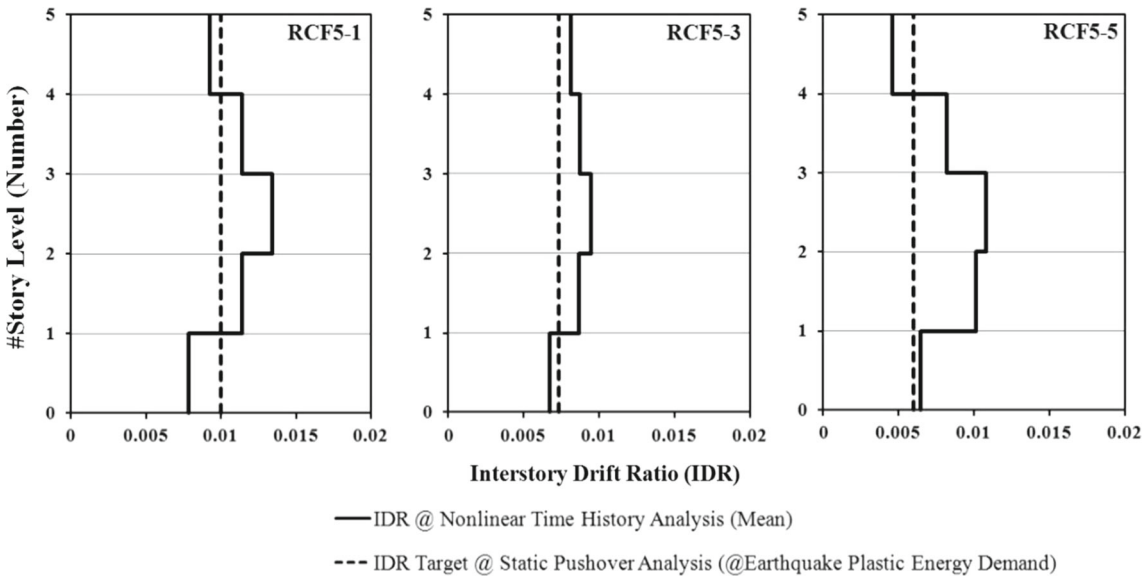

Fig. 23 Interstory drift ratio (*IDR*) results

earthquakes. This leads to approximate $E_{p,max}$ from nonlinear static analysis. The top-left point of the shaded area corresponds to yield base shear force and yield displacement of the frame, while the right border of the same area is determined as to satisfy the mean plastic energy values. Considering the right border displacement of the shaded area under the pushover curve, interstory drift ratios (*IDR*) of the frames are calculated and are compared with those mean *IDR* values obtained from NLTH analysis. The results of this comparison and story-drift profile of frames are given in Fig. 23. While relatively large drifts in middle stories of frames are obtained from NLTH analyses, the interstory drift ratios in the first and the last story are found to be quite close.

5 Conclusions

In the presented study, NLTH analyses of three five-story RC frame structures are performed and the plastic energy dissipated in each frame during the selected earthquakes is determined in a graphical way. The contribution of beam and column deformations to the total plastic energy dissipated in RC frame structure for each time instant of the selected earthquakes is investigated. It can be concluded that rotational deformations of beam plastic hinges make significant contribution to the total plastic energy dissipated in the frame. At the initial time of the earthquakes, plastic hinges generally form in beam members, as is expected, and the most contribution to the total plastic energy comes from plastic deformations of beam hinges. Then plastic hinges form in column members and cyclic behavior of columns start to contribute to the total plastic energy dissipation, while the contribution due to cyclic behavior of beams shows a lower tendency at this stage. It is observed that in some cases, axial plastic deformations of columns also contribute substantially to the total plastic energy dissipated in the frame. The contribution ratios of rotational deformations of beam and column plastic hinges and the contribution of axial deformations of column plastic hinges to the total plastic energy dissipation vary with characteristics of earthquakes.

The correlation of the plastic energy dissipated in beam members with the total plastic energy dissipated in 5-story frame structures is investigated, and a linear model is fitted using regression analysis. Relatively high values of the coefficient of determination are obtained, and linear regression equations, which show the relationship between the plastic energy dissipated in frame and the contribution rotational deformations of beam plastic hinges, are derived. The derived linear equations can be used as simple formulas in order to estimate the total plastic energy dissipated in regular RC frame structures having similar sequence of hinge formation. For frames having different plastic hinge mechanism, the same linear relation may not be obtained.

The lateral top displacement of the selected frames is obtained by equating the area under the pushover curves to the mean values of the maximum plastic energy dissipated in frames during the selected earthquakes. Assuming frames have a certain interstory drift ratio for this plastic energy, interstory drift ratios of the frames are calculated and are compared with those obtained from NLTH analysis. Pushover-based interstory drift ratios are found to be quite close to the drift results of NLTH analysis in the first and the last story of all frames. *IDR* values in middle stories do not match, and relatively large drifts are obtained from NLTH analysis in comparison with pushover analysis.

The contribution ratio of beam and column plastic hinges to the total plastic energy dissipated in nonlinear behavior of RC frames is determined under certain assumptions. The assumptions of NLTH analysis may also effect the accuracy of the plastic energy computations. Additionally, the amount of dissipated plastic energy may vary due to the idealization of moment–rotation relations of structural elements. It is obvious that each ground motion record reflects its own characteristics to NLTH analysis. Consequently, also depending on plastic hinge formation, different contribution ratios of structural members to total dissipated plastic energy may be obtained under different earthquakes.

References

1. Bertero, V.V.; Gilmore, A.T.: Use of energy concepts in earthquake resistant analysis and design: issues and future directions. Advances in Earthquake Engineering Practice. Short Course in Structural Engineering, Architectural and Economic Issues, University of California, Berkeley, CA (1994)
2. Akbas, B.; Shen, J.: Earthquake resistant design and energy concepts. Technical Journal- Digest **2003**, 865–888 (2003). (in Turkish)
3. Housner, G.W.: Limit design of structures to resist earthquakes. In: Proceedings of the 1st World Conference on Earthquake Engineering. Berkeley, CA (1956)
4. Berg, G.V.; Thomaides, S.S.: Energy consumption by structures in strong-motion earthquakes. In: Proceedings of the 2nd World Conference on Earthquake Engineering, pp. 681–696. Tokyo and Kyoto (1960)
5. Ohno, T.; Nishioka, T.: An experimental study on energy absorption capacity of columns in reinforced concrete structures. Proc. JSCE Struct. Eng./Earthq. Eng **1**(2), 23–33 (1984)
6. Uang, C.M.; Bertero, V.V.: Use of energy as a design criterion in earthquake-resistant design. Report No. UCB/EERC-88/18, Earthquake Engineering Research Center, University of California, Berkeley, CA (1988)
7. Léger, P.; Dussault, S.: Seismic-energy dissipation in MDOF structures. J. Struct. Eng. **118**(5), 1251–1269 (1992)
8. Cruz, A.M.F.; López, O.A.: Plastic energy dissipated during an earthquake as a function of structural properties and ground motion characteristics. Eng. Struct. **22**(7), 784–792 (2000)
9. Teran-Gilmore, A.; Avila, E.; Rangel, G.: On the use of plastic energy to establish strength requirements in ductile structures. Eng. Struct. **25**(7), 965–980 (2003)
10. Estes, K.R.: An Energy Method for Seismic Design. Ph.D. Thesis. University of Southern California, California (2003)
11. Khashaee, P.; Mohraz, B.; Sadek, F.; Lew, H.S.; Gross, J.L.: Distribution of earthquake input energy in structures. The National Institute of Standards and Technology (NIST), NISTIR 6903, Building and Fire Research Laboratory, USA (2003)
12. Estes, K.R.; Anderson, J.C.: Earthquake resistant design using hysteretic energy demands for low rise buildings. In: Proceedings of the 13th World Conference on Earthquake Engineering, Paper No. 3276. Vancouver (2004)
13. Kwak, H.; Kim, S.P.; Kim, J.E.: Nonlinear dynamic analysis of RC frames using cyclic moment–curvature relation. Struct. Eng. Mech. **17**(3–4), 357–378 (2004)
14. Lei, C.; Xianguo, Y.; Kangning, L.: Analysis of seismic energy response and distribution of RC frame structures. In: Proceedings of the 14th World Conference on Earthquake Engineering. Beijing, (2008)
15. Kalkan, E.; Kunnath, S.K.: Relevance of absolute and relative energy content in seismic evaluation of structures. Adv. Struct. Eng. **11**(1), 17–34 (2008)

16. Jiang, Y.; Gang, L.; Yang, D.: A modified approach of energy balance concept based multimode pushover analysis to estimate seismic demands for buildings. Eng. Struct. **32**(5), 1272–1283 (2010)
17. Benavent-Climent, A.; López-Almansa, F.; Bravo-González, D.A.: Design energy input spectra for moderate-to-high seismicity regions based on Colombian earthquakes. Soil Dyn. Earthq. Eng. **30**(11), 1129–1148 (2010)
18. Terapathana, S.: An Energy Method for Earthquake Resistant Design of RC Structures. Ph.D. Thesis. University of Southern California, California (2012)
19. Massumi, A.; Monavari, B.: Energy based procedure to obtain target displacement of reinforced concrete structures. Struct. Eng. Mech. **48**(5), 681–695 (2013)
20. Habibi, A.; Chan, R.W.K.; Albermani, F.: Energy-based design method for seismic retrofitting with passive energy dissipation systems. Eng. Struct. **46**, 77–86 (2013)
21. Enderami, S.A.; Beheshti-Aval, S.B.; Saadeghvaziri, M.A.: New energy based approach to predict seismic demands of steel moment resisting frames subjected to near-fault ground motions. Eng. Struct. **72**, 182–192 (2014)
22. Eom, T.S.; Park, H.G.: Evaluation of energy dissipation of slender reinforced concrete members and its applications. Eng. Struct. **32**(9), 2884–2893 (2010)
23. Jiao, Y.; Yamada, S.; Kishiki, S.; Shimada, Y.: Evaluation of plastic energy dissipation capacity of steel beams suffering ductile fracture under various loading histories. Earthq. Eng. Struct. Dyn. **40**(14), 1553–1570 (2011)
24. Lu, X.; Lu, X.; Sezen, H.; Ye, L.: Development of a simplified model and seismic energy dissipation in a super-tall building. Eng. Struct. **67**, 109–122 (2014)
25. Korol, R.M.; Sivakumaran, K.S.: Reassessing the plastic hinge model for energy dissipation of axially loaded columns. J. Struct. **2014**, 1–7 (2014)
26. Acun, B.: Energy Based Seismic Performance Assessment of Reinforced Concrete Columns. Ph.D. Thesis. Middle East Technical University, Ankara (2010)
27. Goel, S.C.; Liao, W.C.; Bayat, M.R.; Chao, S.H.: Performance-based plastic design (PBPD) method for earthquake-resistant structures: an overview. Struct. Design Tall Spec. Build. **19**(1–2), 115–137 (2010)
28. Liao, W.C.: Performance-Based Plastic Design of Earthquake Resistant Reinforced Concrete Moment Frames. Ph.D. Thesis. University of Michigan, Ann Arbor (2010)
29. Kazantzi, A.K.; Vamvatsikos, D.: A study on the correlation between dissipated hysteretic energy and seismic performance. In: Proceedings of the 15th World Conference on Earthquake Engineering. Lisbon (2012)
30. Bai, J.; Ou, J.: Plastic limit-state design of frame structures based on the strong-column weak-beam failure mechanism. In: Proceedings of the 15th World Conference on Earthquake Engineering. Lisbon (2012)
31. Liao, W.C.; Goel, S.C.: Performance-based plastic design and energy-based evaluation of seismic resistant RC moment frame. J. Mar. Sci. Technol. **20**(3), 304–310 (2012)
32. Dindar, A.A.; Yalçın, C.; Yüksel, E.; Özkaynak, H.; Büyüköztürk, O.: Development of earthquake energy demand spectra. Earthq. Spectra **31**(3), 1667–1689 (2015)
33. Mezgebo, M.G.; Lui, E.M.: Hysteresis and soil site dependent input and hysteretic energy spectra for far-source ground motions. Adv. Civil Eng. **2016**, 1–29 (2016)
34. Hernández-Montes, E.; Aschheim, M.A.; Gil-Martin, L.M.: Energy components in nonlinear dynamic response of SDOF systems. Nonlinear Dyn. **82**(1), 933–945 (2015)
35. Akbaş, B.; Akşar, B.; Doran, B.; Alacalı, S.: Hysteretic energy to energy input ratio spectrum in nonlinear systems. J. Sci. Eng. **18**(2), Issue 53, 239–254 (2016)
36. TSDC: Turkish Seismic Design Code. Ministry of Public Works and Settlement, Ankara (2007)
37. UBC: Uniform Building Code. International Conference of Building Officials, Whittier, California (1997)
38. Eurocode 8: Design of structures for earthquake resistance—Part 1: General Rules, Seismic Actions and Rules for buildings, European Committee for Standardization, Brussels (2004)
39. TS500: Requirements for Design and Construction of Reinforced Concrete Structures. Turkish Standards Institute, Ankara (2000)
40. SAP2000: Integrated Structural Analysis and Design Software, Version 15.1.0. Computers and Structures Inc., Berkeley, CA (2011)
41. PERFORM 3D: Nonlinear Analysis and Performance Assessment for 3D Structures, Version 4. Computers and Structures Inc., Berkeley, CA (2009)
42. Mander, J.B.; Priestley, M.J.N.; Park, R.: Theoretical stress–strain model for confined concrete. J. Struct. Eng. **114**(8), 1804–1826 (1988)
43. Clough, R.W.: Effect of stiffness degradation on earthquake ductility requirements. Report No. 66-16, Dept. of Civil Engineering, University of California, Berkeley, CA (1966)
44. Clough, R.W.; Johnston, S.B.: Effect of stiffness degradation on earthquake ductility requirements. In: Proceedings of the Japan Earthquake Engineering Symposium, Tokyo, pp. 227–232 (1966)
45. Takeda, T.; Sozen, M.A.; Nielsen, N.N.: Reinforced concrete response to simulated earthquakes. J. Struct. Div. **96**(12), 2557–2573 (1970)
46. Miranda, E.; Garcia-Ruiz, J.: Influence of stiffness degradation on strength demands of structures built on soft soil sites. Eng. Struct. **24**(10), 1271–1281 (2002)
47. Medina, R.A.; Krawinkler, H.: Influence of hysteretic behavior on the nonlinear response of frame structures. In: Proceedings of the 13th World Conference on Earthquake Engineering. Vancouver, B.C. (2004)
48. Priestley, M.J.N.; Calvi, G.M.; Kowalsky, M.J.: Direct displacement-based seismic design of structures. In: Proceedings of the NZSEE Conference, Paper No. 18, pp. 1–23 (2007)
49. Pacific Earthquake Engineering Research Center: Strong Ground Motion Database. http://ngawest2.berkeley.edu/ (2015). Accessed 15 September 2015
50. Chopra, A.K.: Dynamics of Structures, Theory and Applications to Earthquake Engineering. Prentice Hall, Upper Saddle River (1995)